

Development and Characterization of Gelatin-Based Bio-Nanocomposite Films Reinforced with Carbon Dots for Enhanced Mechanical and Optical Properties

Prima Soheti^{1*}, Charlena¹, Noviyana Darmawan^{1,3}, Mala Nurilmala^{2,3}

¹Department of Chemistry, Faculty of Mathematics and Natural Sciences, IPB University, Bogor, 16680, Indonesia

²Department of Aquatic Product Technology, Faculty of Fisheries and Marine Sciences, IPB University, Bogor, 16680, Indonesia

³Halal Science Center, IPB University, Bogor, 16129, Indonesia

*Email: prima@tau.ac.id

Article Info

Received: Nov 21, 2025
Revised: Apr 10, 2026
Accepted: Apr 19, 2026
Online: May 31, 2026

Citation:

Soheti, P., Charlena, Darmawan, N., Nurilmala, M. (2026). Development and Characterization of Gelatin-Based Bio-Nanocomposite Films Reinforced with Carbon Dots for Enhanced Mechanical and Optical Properties. *Jurnal Kimia Valensi*, 12(1), 35-48.

Doi:

[10.15408/jkv.v12i1.48995](https://doi.org/10.15408/jkv.v12i1.48995)

Abstract

Gelatin-based bio-nanocomposite films reinforced with carbon dots were developed and characterized to evaluate their mechanical, thermal, and optical properties. The films were prepared with carbon dot concentrations of 0.0, 0.1, 0.5, and 1.0% (w/w) to examine the effect of nanofiller incorporation. Optical analysis showed enhanced ultraviolet-visible absorption at 339–344 nm and red-shifted fluorescence emission at 500–517 nm under 400 nm excitation, indicating improved light-responsive behavior. The addition of carbon dots significantly improved tensile strength, elongation at break, and Young's modulus, demonstrating enhanced flexibility and mechanical performance. Furthermore, carbon dots reduced the water vapor transmission rate and transparency while increasing film density, indicating improved barrier properties. The film containing 0.5% carbon dots showed the most balanced performance, with a tensile strength of 27.43 ± 0.71 MPa, elongation at break of $23.17 \pm 1.66\%$, and Young's modulus of 0.26 ± 0.03 GPa. Structural analysis confirmed no significant changes in chemical composition and showed uniform dispersion of carbon dots. Thermal analysis indicated improved stability with a melting temperature of 167°C . These findings highlight the potential of gelatin-based bio-nanocomposite films for sustainable packaging applications.

Keywords: Bio-nanocomposites, carbon dots, films, gelatin

1. INTRODUCTION

Gelatin as protein biopolymers has been studied extensively in the pharmaceutical field as a capsule shell material¹, wound treatment and drug delivery², and biodegradable films as a substitute for petroleum polymers³. Gelatin is biocompatible, non-immunogenic, low gelling temperature, low melting point, and has good gas barrier capacity^{4,5}. Gelatin is also reported to have a high abundance, so its utilization is essential to increase its commercial value. The utilization of gelatin which is readily decomposed or biodegradable can prevent environmental pollution⁶. However, gelatin made into films is known to have inferior mechanical properties, water barrier characteristics, and thermal properties that limit its use^{7,8}.

Adding of nano-sized fillers or nanofillers at low concentrations to nanocomposites can enhance the mechanical and thermal properties of polymers⁹. Because of their high surface energy and expanded surface area, film fillers with a minimum of one nano-size dimension (nanofillers) have superior interfacial interactions with the polymer matrix than micro- or macro-fillers. It will greatly improve the polymer's mechanical characteristics¹⁰. Various nanofillers such as ZnO⁴, CuS¹¹, and Ag-Cu¹² have been reported to enhance the mechanical and thermal properties of gelatin-based bio-nanocomposite films.

An alternative nanofiller for gelatin-based films is carbon dots (C-dots), which are nanoscale carbon particles with sizes generally below 10 nanometers and are characterized by strong light emission, large surface area, and abundant functional groups such as

hydroxyl, carboxyl, and amino groups that facilitate strong interactions with gelatin matrices, thereby improving film structure and mechanical performance^{2,13}. Previous studies on gelatin-based nanocomposite films have mainly utilized inorganic fillers such as ZnO, CuS, and Ag-Cu nanoparticles to enhance mechanical strength and antimicrobial properties. However, these materials may present limitations, including potential toxicity, particle aggregation, and reduced transparency. In contrast, C-dots exhibit better compatibility with polymer matrices, improved dispersion, and additional optical functionalities such as light emission and ultraviolet absorption while maintaining film clarity, although their antimicrobial activity is generally lower than that of metal-based fillers^{10,14}.

Moreover, C-dots have been reported to enhance mechanical properties, including tensile strength and elongation, in various polymer systems such as carboxylated styrene-butadiene rubber (XSBR)¹⁵, polyvinylpyrrolidone (PVP), and polyethersulfone (PES)¹⁶. Composite membranes of polyacrylonitrile (PAN)/C-dots have shown improved tensile strength and Young's modulus values¹⁷. These nanoparticles are typically synthesized from carbon sources such as citric acid combined with surface passivating agents including polyethylene diamine¹⁸, ethylenediamine¹⁹, urea²⁰, or glutathione²¹. In addition, C-dots are known for their good biocompatibility, chemical stability, low toxicity, ease of surface modification, cost-effective synthesis, and abundant raw materials²². C-dots have been widely explored in applications such as optical sensors²³, photocatalysts²⁴, corrosion inhibitors²⁵, bioimaging¹⁹, and the development of intelligent packaging systems, making them promising candidates for multifunctional and sustainable bio-nanocomposite films²⁶.

Furthermore, gelatin-based bio-nanocomposite films incorporating C-dots, including systems such as gelatin-based nanocomposite hydrogel²⁷ and hybrid biobased films have attracted increasing attention due to their biodegradability, excellent film-forming ability, and tunable multifunctional properties. Previous studies have primarily focused on improving individual characteristics, such as mechanical strength, barrier performance, or optical properties, through the incorporation of C-dots into gelatin matrices²⁸. However, comprehensive studies that systematically correlate structural interactions with mechanical and optical performance remain limited and are not yet fully understood.

In this study, gelatin/C-dots bio-nanocomposite films were developed to elucidate the interfacial interactions between gelatin and C-dots and their influence on film properties. The novelty of this work lies in the systematic evaluation of the role of C-dots as functional nanofillers in enhancing both mechanical

and optical properties, providing deeper insight into the structure–property relationships within the gelatin matrix. Therefore, this study aims to investigate the effect of varying gelatin/C-dots ratios on the physicochemical and functional characteristics of the films, including thickness, density, water vapor transmission rate (WVTR), transparency, morphology, functional groups, thermal stability, and mechanical properties (tensile strength, elongation at break, and Young's modulus). Additionally, the fluorescence-related optical properties are explored to highlight the potential of these films for future smart packaging applications.

2. RESEARCH METHODS

Materials

The chemicals used are bovine gelatin (30 Mesh, 150 Bloom/Global Capsules), glycerol (P and G Chemicals), urea (Merck), and citric acid (Pudak Scientific). The instruments used are a Pycnometer (Pyrex), Micrometer (Mitutoyo Manufacturing), Mechanical Universal Testing Machine (Testometric FS500AT), Universal Attenuated Total Reflection-Fourier Transform Infrared (UATR-FTIR) (Spectrum Two Perkin Elmer), Scanning Electron Microscopy (SEM) (Carl Zeiss EVO MA 10), Thermal Gravimetry-Differential Scanning Calorimetry (TG-DSC) (200-F3 Maia), UV-Vis spectrophotometer (1700 Shimadzu), and spectrofluorometer (F-2700 FL Spectrophotometer).

Synthesis of C-dots Nanoparticles

C-dots were synthesized by dissolving 2.6 g of citric acid and 1.4 g of urea in 20 mL of distilled water, followed by heating in a 700 W microwave for 5 minutes. This process yielded a dark brown solid product, corresponding to C-dots. The obtained solid was subsequently redispersed in 100 mL of demineralized water, thoroughly mixed, and centrifuged at 3000 rpm for 20 minutes to remove large aggregates. The resulting supernatant was then filtered through a 0.2 μm membrane to obtain a clear brown solution with a C-dots concentration of 1 mg/mL. The prepared solution was stored at 4°C prior to further use^{20,29,30}.

Fabrication of Gelatin/C-dots Bio-nanocomposite Films

A gelatin solution comprising 4 g of gelatin was dissolved in 100 mL of distilled water before being heated at 45 °C for 30 minutes while stirring continuously. As a plasticizer, 0.95 mL of glycerol was added due to its high compatibility with gelatin and its ability to form hydrogen bonds with polymer chains, thereby improving film flexibility and reducing brittleness. The solution was warmed and agitated for 15 minutes at 45°C. Various

concentrations of C-dots (0, 0.1, 0.5, and 1% w/w) were added and the solution was mixed slowly for 60 minutes. The solution was then poured into a glass plate (15 x 15 x 1 cm) and allowed to dry for three days at 23-25°C^{8,31}.

Film Thickness

At three random locations around the film, the thickness was measured with a micrometer (0.001 mm). The film thickness was calculated using the average value³².

Film Transparency

A UV-Vis spectrophotometer was used to measure the film's transparency at a wavelength (λ) of 550 nm. The known thickness (x mm) film was cut sufficiently and then put into the test cell. Film transparency (mm^{-1}) was calculated based on the equation³ :

$$T = \frac{\text{The Absorbance at 550 nm}}{\text{Film thickness (mm)}} \quad (1)$$

Film Density

Density measurements were carried out using a pycnometer. The density value is calculated based on the equation³³ :

$$ds = \frac{(mps - mp) \times d1}{mpl - mp - mpls + mps} \quad (2)$$

Where ds is density of film (g/cm^3), mp is empty weight of pycnometer (g), mps is pycnometer weight + sample (g), mpl is pycnometer weight + water (g), mpls is pycnometer weight + sample + water (g). At 23- 27°C, d1 is the density of the immersion liquid (g/cm^3).

Water Vapour Transmission Rate (WVTR) Test

The 4 x 4 cm film sample was placed in a test cup filled with 10 mL of distilled water. After that, the entire system (test cup + water + film) was placed in a desiccator. The mass of the system was measured hourly for a total of 3 hours. The WVTR value of the sample is calculated using the equation^{32,34} :

$$\text{WVTR} = \frac{\text{weight loss (g)}}{\text{film area (cm}^2\text{) x time (hour)}} \quad (3)$$

Scanning Electron Microscopy (SEM)

The film sample was dried in a desiccator for two weeks before being placed in a double-adhesive set holder. The gold coating was then coated on the sample in a vacuum and evaluated by SEM at higher magnification (5000x)⁴.

Universal Attenuated Total Reflectance–Fourier Transform Infrared (UATR-FTIR) Analysis

UATR-FTIR was used to record the FTIR spectrum of the C-dots samples and bio-nanocomposite films, ranging from 400 to 4000 cm^{-1} . The test results are in the form of a spectrum that is then interpreted, including the wavenumber and percent transmittance to determine the functional group¹².

Mechanical Properties

Mechanical Universal Testing Machine equipped with a load cell of 60 N is used to determine the tensile strength, elongation, and Young's modulus. Before testing, the films were conditioned for 48 hours at $23 \pm 2^\circ\text{C}$. A mechanical crosshead speed of 30 mm/min was used to test the films³⁵.

Thermogravimetric–Differential Scanning Calorimetry (TG-DSC) Analysis

TG-DSC was used to determine the thermal characteristics of the films. The samples were conditioned in a desiccator for one week at 23-25°C. The sample was then encapsulated on an aluminium plate and scanned at 30-500°C at a 10°C/min heating rate. As a reference, a blank aluminium plate was used⁴.

Optical Properties

The optical properties of the films were determined by analyzing their UV-Vis absorption spectrum and fluorescence emission spectra. UV–VIS absorption spectrum of film in a 200–800 nm range was recorded using a UV–VIS spectrometer. A spectrofluorometer measured the fluorescence emission spectrum of the film at an excitation wavelength of 400 nm³⁶.

Statistical Analysis

Data were processed and analyzed using statistical analysis of variance (ANOVA) and Tukey's multiple comparison tests with a confidence interval of 0.05. The data were then shown as mean \pm standard deviation (N=3), significant differences indicated by different letters at $p < 0.05$. Minitab 18 was used to conduct the statistical analysis⁴.

3. RESULTS AND DISCUSSION

Physical Appearance of Gelatin/C-dots Bio-nanocomposite Films

The homogeneous distribution of the nanofiller significantly influences the physical appearance of the film³⁷. Gelatin films typically exhibit a smooth and flexible surface with a translucent to transparent appearance (**Figure 1a**)^{5,38}. These transparent properties are obtained from the homogeneous

dispersion of the components within the matrix. The film color changed upon light exposure depending on the concentration of the brownish C-dots solution incorporated into the bio-nanocomposite films, as shown in **Figures 1b – 1d**. The resulting film appearance was systematically compared with previous studies on gelatin-based bio-nanocomposite films incorporating other nanofillers, such as ZnO⁷, Ag–Cu¹², and Multi Walled Carbon Nanotubes (MWCN)³⁹. The developed gelatin/C-dots bio-nanocomposite films exhibited improved visual homogeneity and transparency, which is consistent

with earlier reports on carbon dot-reinforced biopolymer films. This enhancement can be attributed to the uniform dispersion of C-dots within the gelatin matrix and the strong interfacial interactions that minimize phase separation and light scattering¹⁷. In contrast, films containing inorganic fillers often exhibit increased opacity due to particle aggregation, whereas the present films maintained a more uniform and clearer structure. These findings are in good agreement with previous studies, confirming that C-dots can effectively improve the visual and optical quality of biopolymer-based films.



Figure 1. Photographs of gelatin/C-dots composite films with various C-dots content a) 0%; b) 0.1%; c) 0.5%; d) 1% under daylight (left) and UV lamp (265 nm, right)

Film Thickness and Transparency

The thickness of the gelatin film in this study did not experience a notable difference with the inclusion of C-dots ($p < 0.05$) (Table 1). The results indicate that film thickness slightly increased with increasing C-dots concentration, which is consistent with earlier reports on nanofiller-reinforced biopolymer films, where the incorporation of nanoparticles contributes to a denser matrix structure^{31,32}. According to Japanese Industrial Standard (JIS Standard)⁴⁰, a film must have a thickness equal to or less than 0.025 mm⁴¹. Thus, the obtained film thickness is suitable for the standard. The film's thickness also affects the transparency value of the film. Transparency is an important physical feature of packaging films which indicates that the films are transparent⁴². The functioning of a film is inextricably linked to its transparency because of its significant influence on the product's appearance, which will be directly proportional to consumer acceptance^{43,44}.

A higher transparency value indicates lower film transparency, and in this study, the transparency of gelatin/C-dots bio-nanocomposite films decreased significantly ($p < 0.05$) with increasing C-dots content (Table 1). This reduction is mainly attributed to the obstruction of light transmission caused by the higher concentration of C-dots nanoparticles, which is consistent with the darker appearance observed at

higher loadings. The effect is further associated with enhanced light absorption arising from the conjugated carbon structure and surface functional groups of C-dots, which introduce additional chromophoric sites and electronic transitions, along with increased light scattering within the film matrix⁴⁵. A similar decrease in transparency has also been reported in gelatin-based bio-nanocomposite films incorporating other nanofillers, such as ZnO, Ag–Cu, and multi-walled carbon nanotubes such as ZnO⁷, Ag–Cu¹², and MWCN³⁹. In this study, the transparency value of the gelatin/C-dots 0.5% (w/w) film was 3.94 ± 0.03 . It is better than the gelatin/Ag–Cu 0.5% (w/w), which was 5.55 ± 0.2^{12} , and the gelatin/MWCN 0.5% (w/w), which was 7 ± 0.54^{39} . The addition of C-dots into the gelatin matrix resulted in a film with better transparency. The homogeneous dispersion of C-dots also affected the film transparency.

Film Density

Film density is an important physical property that indicates the compactness of the bio-nanocomposite structure, which is closely related to its mechanical strength and barrier performance⁴⁶. The density of the gelatin/C-dots bio-nanocomposite film showed a significant difference ($p < 0.05$) at different C-dots concentrations (**Table 1**). The gelatin/C-dots film increased the density value up to 60.33%. An

increased density value was also reported in gelatin films with tara gum added⁴⁷. The inclusion of carbon nanotubes in the graphene composite film also enhanced the density values⁴⁸. The increased density of films was associated with the presence of C-dots as a nanofiller in the gelatin film matrix. The intense interaction between the nanofillers forms a solid interfacial adhesion with the film matrix⁴⁹. This will result in a reduced free volume in the gelatin biopolymer. The gelatin/C-dots bio-nanocomposite film structure is denser than the gelatin film without adding C-dots.

Water Vapour Transmission Rate (WVTR)

The water vapor transmission rate (WVTR) is widely employed to characterize the moisture barrier properties of bio-nanocomposite films⁵⁰. This parameter quantifies the rate at which water vapor permeates through the bio-nanocomposite film matrix⁵¹. WVTR is important because it is related to a critical parameter to ensure the organoleptic quality of food, namely shelf life⁵². One of the primary roles of food packaging in the food industry is to prevent or limit moisture transfer between the food and the environment. Hence the water vapour transmission

rate (WVTR) should be as low as possible. The WVTR value depends on the simultaneous action of water diffusion and its solubility in the polymer matrix³⁴.

Table 1 presents the WVTR values obtained in this study. The WVTR of the gelatin/C-dots film decreased significantly by up to 45.01% compared to the control gelatin film ($p < 0.05$), indicating that the incorporation of C-dots nanoparticles effectively reduces water vapor transmission through the gelatin matrix. This reduction can be attributed to the barrier effect of the C-dots nanoparticles, which are homogeneously dispersed within the gelatin polymer matrix, thereby hindering moisture diffusion. Moreover, the incorporation of nanoparticles increases the tortuosity of the diffusion pathways, forcing water molecules to follow longer and more complex routes through the film matrix, which further contributes to the decrease in WVTR⁵³. Consequently, the reduced WVTR suggests that the gelatin/C-dots bio-nanocomposite film can effectively limit water vapor migration, potentially supporting the maintenance of food quality during storage and highlighting its suitability for potential active packaging applications.

Table 1. Mechanical properties, transparency, density, and water vapor transmission rate of gelatin and gelatin/C-dots films

C-dots contents	Thickness (mm)	Transparency (mm^{-1})	Tensile Strength (MPa)	Elongation at Break (%)	Young's Modulus (GPa)	Density (g/cm^3)	WVTR ($\text{g/m}^2 \text{h}$)
0	0.02 ± 0.002^a	0.80 ± 0.03^d	20.15 ± 0.68^c	18.31 ± 0.72^b	0.19 ± 0.07^b	1.21 ± 0.002^d	40.46 ± 0.13^a
0.1%	0.02 ± 0.001^a	3.07 ± 0.03^c	22.75 ± 1.48^b	20.32 ± 1.54^{ab}	0.09 ± 0.06^b	1.44 ± 0.003^c	28.50 ± 0.11^b
0.5%	0.02 ± 0.003^a	3.94 ± 0.03^b	27.43 ± 0.71^a	23.17 ± 1.66^a	0.26 ± 0.03^{ab}	1.72 ± 0.004^b	26.06 ± 0.17^c
1%	0.02 ± 0.001^a	7.75 ± 0.05^a	28.79 ± 0.53^a	17.19 ± 1.77^b	0.40 ± 0.12^a	1.94 ± 0.002^a	22.25 ± 0.13^d

For each film, the reported values are the mean \pm standard deviation. According to the Tukey test (N=3), the values mean followed by a distinct letter are significantly ($p < 0.05$) different.

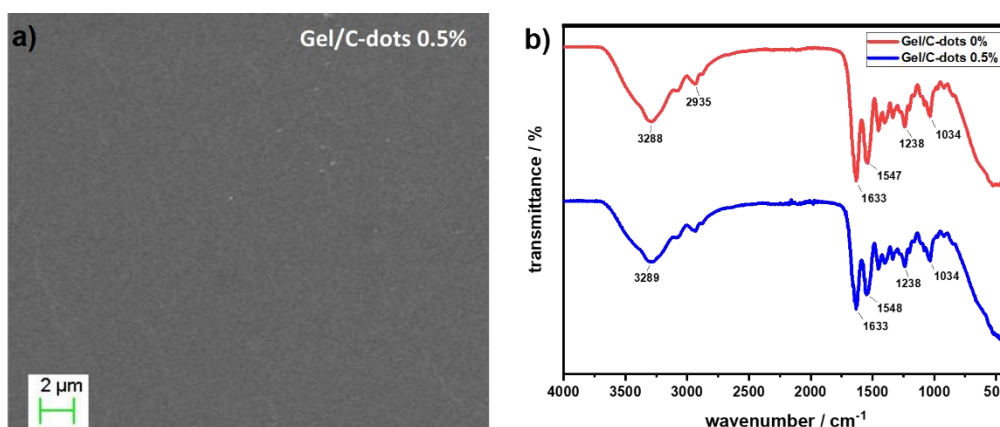


Figure 2. a) SEM micrograph b) FTIR spectrum of gelatin/C-dots films

Morphology of Gelatin/C-dots Bio-nanocomposite Film

The gelatin/C-dots bio-nanocomposite film exhibited a smooth and homogeneous surface without

visible cracks or deformation, as shown in **Figure 2a**. The incorporation of 0.5% (w/w) C-dots resulted in a uniform distribution of nanoparticles throughout the gelatin matrix, leading to a relatively dense film

structure. This dense morphology suggests strong interfacial interactions between the nanoparticles and the polymer matrix, which can account for the enhanced mechanical properties of the bio-nanocomposite films^{8,54}. The absence of aggregation further indicates high compatibility between C-dots and gelatin, likely arising from electrostatic interactions associated with the anionic and cationic functional groups present in both the biopolymer matrix and the nanofiller⁵⁵. Moreover, a homogeneous morphology of gelatin/C-dots film contributes to the stability of the film's physical properties, an essential criterion for commercial packaging applications.

Functional Groups of Gelatin/C-dots Bio-nanocomposite Film

An FTIR spectroscopic study was used to further characterize the influence of C-dots fillers on the structure of the gelatin matrix, as shown in **Figure 2b**. The dominant peak at 1633 cm^{-1} , which is the typical peak of amide-I, can be seen in all of the films' FTIR spectra. It is connected to the C=O/hydrogen bond strain and the COO group (amide-I, C=O stretching)⁷. Peak in the gelatin film was detected at a wavenumber of 3288 cm^{-1} is amide-A associated with OH and NH stretching vibrations of gelatin (amide-A, NH stretching)⁵⁶. The typical band around 2935 cm^{-1} is caused by the alkane group's CH stretching vibration (CH stretching vibration) in the gelatin polymer chain. Peaks at 1547 cm^{-1} (amide-II, NH bending) and 1238 cm^{-1} (amide-III, C-N, and NH stretching) were also identified¹¹. All film samples included bands with wavenumbers of 1034 cm^{-1} , indicating that glycerol (-OH group) was used as a plasticizer⁵⁷.

The FTIR spectra of the gelatin and gelatin/C-dots (0.5% w/w) bio-nanocomposite films exhibited similar characteristic peaks, with only slight variations in peak intensity, indicating that the incorporation of C-dots did not alter the fundamental chemical structure of the gelatin matrix. The addition of C-dots resulted in minor shifts of specific absorption bands, particularly at 3289 cm^{-1} and 1548 cm^{-1} , toward higher wavenumbers. As shown in **Figure 2b**, these shifts in the amide-A and amide-II bands can be attributed to the formation of hydrogen bonding interactions between the gelatin matrix and the C-dots nanoparticles, likely involving weak intermolecular forces such as van der Waals interactions¹¹. Functional groups present in gelatin, including -OH and -NH₂, can interact with corresponding -OH and -NH₂ groups on the surface of C-dots, leading to the observed spectral shifts^{4,58}. These findings confirm the presence of intermolecular interactions between gelatin and C-dots, as evidenced by FTIR analysis, which contribute to the structural stability and sustained bioactive functionality of the bio-nanocomposite films during

application. Although no significant spectral differences were observed among the samples, FTIR plays a crucial role in verifying the presence of key functional groups and their interactions within the matrix. This information complements the morphological and elemental analyses obtained from SEM by providing molecular-level insight into the chemical structure, thereby enabling a more comprehensive understanding of the structure-property relationships in the developed bio-nanocomposite films.

Mechanical Properties

Mechanical properties such as tensile strength, elongation, and Young's modulus, are essential properties of packaging films to withstand external stresses while maintaining their integrity⁵¹. Good mechanical properties can ensure the film's integrity during handling, processing, and shipping or protect the film from minor defect formation^{59,60}. **Figure 3a** depicts a typical stress-strain curve for the film. When stress increases rapidly with increased strain, this curve demonstrates typical deformation behaviour at low strain (10%). When the stress level exceeds 10%, the stress level rises until failure occurs. This curve shows that the inclusion of C-dots into the gelatin film causes the stress and strain of the film to change. Stress and strain also increase with increasing C-dots in the film. It indicates that the gelatin/C-dots bio-nanocomposite film has better mechanical properties (increased strength and flexibility) than the gelatin film without the addition of C-dots.

In this study, the gelatin/C-dots bio-nanocomposite film had a better tensile strength value than the gelatin film without adding C-dots (Table 1). The tensile strength of the gelatin film without adding C-dots was $20.153 \pm 0.675\text{ MPa}$, but when C-dots was added at 0.5% (w/w). It increased significantly ($p < 0.05$) to $27.432 \pm 0.706\text{ MPa}$. However, the increase in tensile strength of 28.792 ± 0.528 was not significant with the addition of 1% (w/w) C-dots. It may be due to the excessive loading of nanoparticles into the gelatin matrix, which disrupts the stability of the matrix so that the gelatin cannot withstand additional nanoparticles¹². According to conventional standards, the packaging film's tensile strength must be greater than 3.5 MPa ⁸ and more than 3.923 MPa based on JIS standards⁴⁰. Meanwhile, the value of the standard tensile strength of LDPE commercial plastic must be more than 23.58 MPa according to ASTM⁶¹. Thus, the tensile strength value of the 0.5% (w/w) gelatin/C-dots bio-nanocomposite film has met the ASTM, JIS, and conventional standards of gelatin/C-dots bio-nanocomposite films as packaging films.

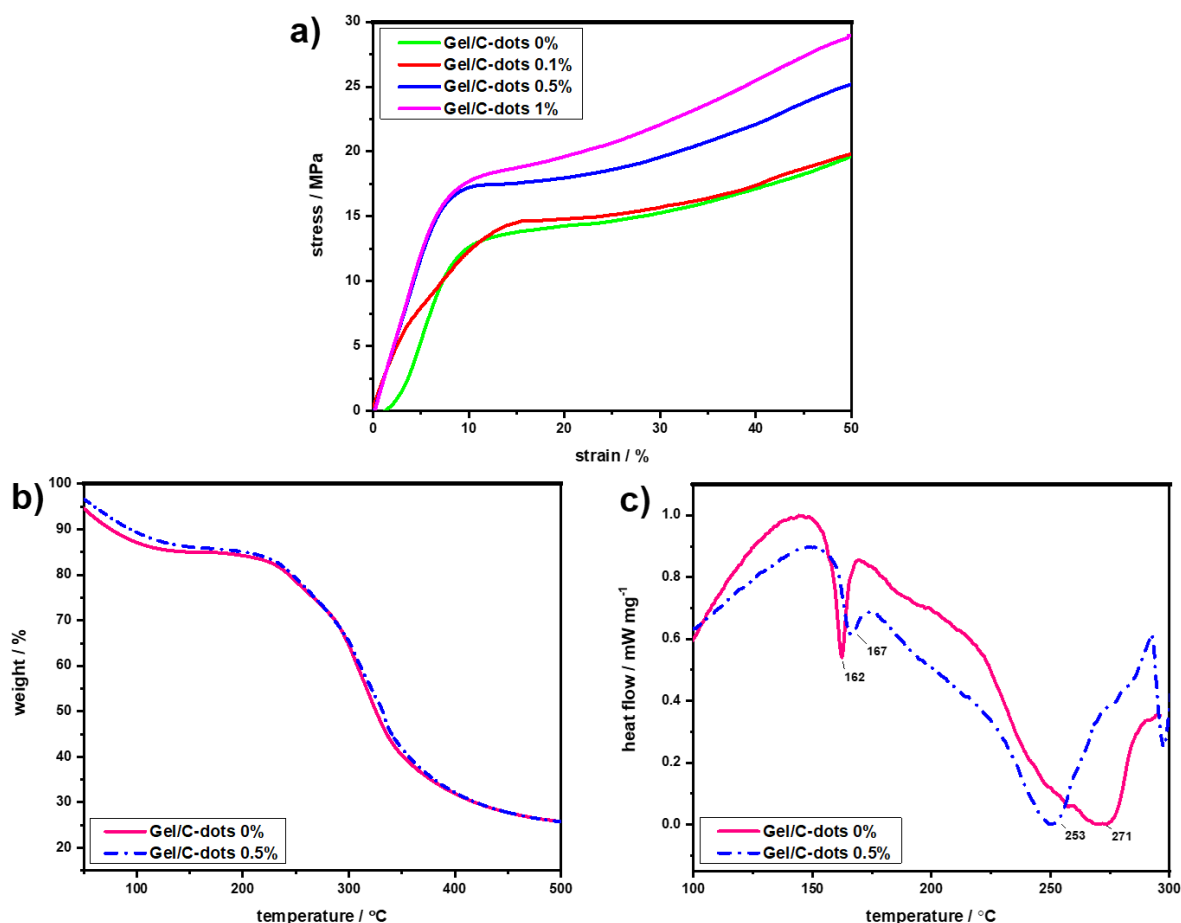


Figure 3. a) Stress-Strain curves b) TGA c) DSC thermograms of gelatin/C-dots films

With the addition of C-dots, the elongation value improved noticeably ($p < 0.05$), but with the addition of 1% (w/w) C-dots, the elongation value declined (Table 1). When C-dots 0.5% (w/w) and 1% (w/w) were added to gelatin film, Young's modulus value ($p < 0.05$) increased significantly, but not significantly, when C-dots 0.1% (w/w) was added (Table 1). The non-uniform distribution of C-dots causes the fluctuating values of elongation and Young's modulus in the film. The film's mechanical properties are ruled by the polymer matrix's intramolecular and intermolecular interactions and distributions⁷.

The interaction between the C-dots nanofiller and the polymer through covalent bonding improves mechanical parameters, including tensile strength and Young's modulus. It improves stress transfer from the polymer matrix to the filler particles, specifically C-dots. Furthermore, the sheer magnitude of the C-dots covalent bonds in the polymer matrix at high stress may increase the elongation value¹⁵. The increase in elongation indicates that the composite film has greater extensibility and flexibility in polymer structure than the gelatin film⁶². The increase in elongation was also found in gelatin nanocomposite

films with the addition of resorcinol/Ag⁶³, clay⁶⁴, and ZnO⁶⁵ nanoparticles.

The observed changes in the mechanical properties of the gelatin/C-dots films indicate effective interfacial molecular interactions between the polymer matrix and the nanofiller at the film surface, contributing to the enhanced strength of the nanocomposite¹¹. The hydrophilic nature of the C-dots promotes improved flexibility and higher tensile stress at break, as previously reported¹⁶. The incorporation of C-dots is also likely to increase polymer chain mobility⁶⁶, resulting in greater extensibility and stretchability of the bio-nanocomposite films. These enhancements can be attributed to intra- and intermolecular interactions within the film network. Similar improvements in mechanical performance have been reported for gelatin-based nanocomposite films containing various nanofillers^{67,68,69}. However, the gelatin/C-dots films developed in this study exhibit comparable mechanical properties despite having a significantly lower thickness (Table 2). Overall, the improvement in tensile strength and flexibility suggests that the gelatin/C-dots films possess strong potential for application as active packaging materials, with sufficient mechanical integrity to withstand food storage and distribution conditions.

Table 2. Mechanical properties of gelatin films with various nanofillers

Gelatin films with various nanofillers	Thickness (μm)	Tensile Strength (MPa)	Elongation at Break (%)	Young's Modulus (GPa)	References
Gelatin (Bovine)	100.0 \pm 5.0 ^a	13.4 \pm 1.2 ^d	95.0 \pm 5.0 ^a	0.05 \pm 0.01 ^c	39
Gelatin/MWCNT 0.5%	100.0 \pm 5.0 ^a	22.6 \pm 3.2 ^{bc}	66.0 \pm 4.7 ^c	0.07 \pm 0.01 ^b	
Gelatin (Bovine)	75.0 \pm 5.5 ^a	25.8 \pm 0.68 ^c	21.4 \pm 5.2 ^a	0.73 \pm 0.04 ^b	63
Gelatin/Resorcinol/AgNP 0.5%	79.8 \pm 5.3 ^a	10.2 \pm 2.8 ^{ab}	71.8 \pm 5.9 ^{cd}	0.07 \pm 0.01 ^a	70
Gelatin (Bovine)	72.0 \pm 3.0 ^a	3.9 \pm 2.4 ^{ab}	33.0 \pm 1.3 ^b	0.34 \pm 0.02 ^a	70
Gelatin/TiO ₂ 0.5%	72.0 \pm 3.0 ^a	2.8 \pm 2.4 ^{bc}	15.0 \pm 1.3 ^{bc}	0.34 \pm 0.02 ^a	
Gelatin (Bovine)/PVA	160.0 \pm 10.0 ^a	14.6 \pm 0.2 ^a	35.8 \pm 0.5 ^a	0.2 \pm 0.0 ^a	71
Gelatin/PVA/4AZ/ZnO 0.5%	180.0 \pm 10.0 ^a	19.8 \pm 0.2 ^b	13.9 \pm 0.2 ^b	0.37 \pm 0.0 ^a	
Gelatin (Bovine)	68.2 \pm 3.7 ^a	33.6 \pm 2.4 ^a	15.0 \pm 4.5 ^b	1.05 \pm 0.08 ^a	7
Gelatin/MNP 0.5%	74.5 \pm 4.5 ^{bc}	46.5 \pm 3.1 ^c	11.8 \pm 2.9 ^a	1.56 \pm 0.10 ^d	
Gelatin (Bovine)	20.0 \pm 1.0 ^a	20.15 \pm 0.68 ^c	18.31 \pm 0.72 ^b	0.19 \pm 0.07 ^b	This Work
Gelatin/C-dots 0.5%	20.0 \pm 1.0 ^a	27.43 \pm 0.71 ^a	23.17 \pm 1.66 ^a	0.26 \pm 0.03 ^{ab}	

Table 3. Thermal properties of gelatin films with various nanofillers

Gelatin films with various nanofillers	First TG decomposition ($^{\circ}\text{C}$)	Second TG decomposition ($^{\circ}\text{C}$)	Third TG decomposition ($^{\circ}\text{C}$)	References
Gelatin (Bovine)	60-120	200-250	310	11
Gelatin/CuS 0.5%	60-120	200-250	323	
Gelatin (Bovine)	80-120	240	310	63
Gelatin/Resorcinol/AgNP 0.5%	80-120	240	310	
Gelatin (Bovine)	90	240-260	320	74
Gelatin/ZnONP 0.5%	90	240-260	320	
Gelatin (Bovine)	80-120	200-300	320	75
Gelatin/GES/TiO ₂ 0.5%	80-120	200-300	320	
Gelatin (Bovine)	50-100	230-280	332	This Work.
Gelatin/C-dots 0.5%	50-100	230-280	332	

Thermostability

The thermal characteristics of the film samples were analyzed using thermogravimetric analysis (TGA) and differential scanning calorimetry (DSC). **Figure 3b** shows the TGA thermogram of the film. The first weight loss occurred at 50-100 $^{\circ}\text{C}$ due to loss of physically absorbed moisture. Due to glycerol degradation, further decomposition began at around 230 $^{\circ}\text{C}$ and reaches a maximum temperature of around 280 $^{\circ}\text{C}$ ⁶³. The third decomposition is due to thermal degradation of the gelatin matrix, observed at 332 $^{\circ}\text{C}$ of the gelatin film and the gelatin/C-dots 0.5% (w/w). Thus, the addition of a low nanoparticle concentration of 0.5% (w/w) did not change the degradation temperature of gelatin^{72,73}. Similar results were also reported on gelatin films with various nanofillers (**Table 3**).

Figure 3c shows the DSC thermogram of the gelatin film and the gelatin/C-dots bio-nanocomposite film. The sample's melting point was determined using the top location at the endothermic peak of the DSC thermogram. Two endothermic peaks in the gelatin

film, at 162 $^{\circ}\text{C}$ and 271 $^{\circ}\text{C}$, indicate this sample's two distinct primary crystal structures. The devitrification of the amino acid-rich block may be linked to the crystals melting at 162 $^{\circ}\text{C}$. Meanwhile, the devitrification of blocks rich in imino acids like proline and hydroxyproline may be linked to the crystallization melting at 271 $^{\circ}\text{C}$ ⁴. The first melting point (first endothermic peak) increased to 167 $^{\circ}\text{C}$ when C-dots was incorporated into the gelatin matrix. However, the second melting point (second endothermic peak) decreased to 253 $^{\circ}\text{C}$. Nanoparticles as nucleating agents for gelatin cause this variation in melting point⁸. Nanoparticles can improve the regularity and cohesiveness of gelatin chains by improving heterogeneous nucleation and the overall crystallinity of polymers. Nanoparticles occupied the free space between neighbouring gelatin chains, influencing the gelatin film's thermal characteristics⁶⁵.

Optical Properties

C-dots nanoparticles were added to the gelatin film to create a bio-nanocomposite film that may emit

fluorescence emission. When a UV lamp irradiated the gelatin/C-dots bio-nano composite film, it illuminated, indicating that the C-dots was well disseminated in the film matrix. At a wavelength of 254 nm, the film

produced with C-dots will emit a blue-green fluorescence emission (Figure 1)²⁰. As the amount of C-dots in the film grew, the emission color produced by the film became increasingly evident.

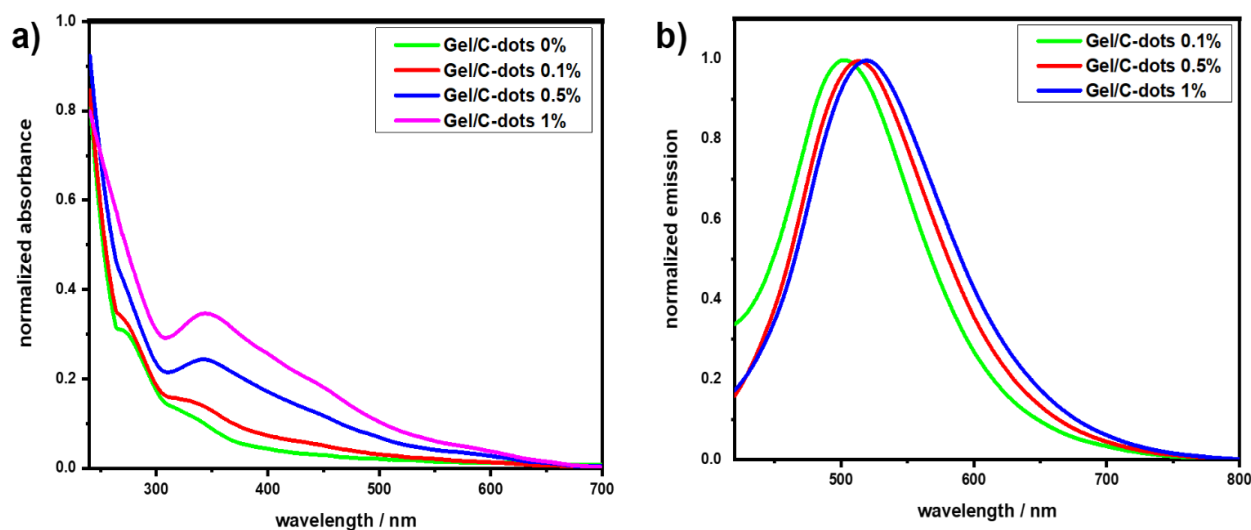


Figure 4. a) UV-vis absorbance spectrum b) Emission spectrum of gelatin/C-dots films

The optical properties of UV-VIS rays are essential in packaging films to protect foodstuffs from photodegradation⁷⁶. As a result, the UV-VIS absorbance spectrum was used to gain information on the optical properties of films (Figure 4a). The pure gelatin film (without adding C-dots) is optically transparent at 200-800 nm. Gelatin molecules showed negligible absorbance or scattering of light in this area of the electromagnetic spectrum. Gelatin-containing thin molecules can induce this effect by forming cross-links (helical areas) much smaller than the wavelength of light. Even so, at wavelengths spanning from 200 to 350 nm, the absorption of UV light by phenolic and other functional groups in gelatin caused the film to become optically opaque⁷⁷

The addition of C-dots to the gelatin matrix resulted in a considerable increase in the film's light absorbance, as seen in Figure 4a⁷⁸. Each gelatin/C-dots bio-nanocomposite film (0.1, 0.5, and 1.0% (w/w)) had an extra absorption peak associated with C-dots absorption at 339, 342, and 344 nm. Gelatin film containing C-dots also experienced increased absorbance intensity even though it had a UV-VIS spectrum similar to gelatin film without C-dots. The absorbance was observed to increase with increasing nanoparticle content in the biopolymer film⁷⁹. The distribution of C-dots nanoparticles and the interaction between C-dots and gelatin are most likely responsible for the increase in light absorption. With different light absorbances, this phenomenon generates changes in the morphology of the film matrix³⁹. This increase in light absorbance makes the gelatin/C-dots bio-nanocomposite film lose its transparency, but the

resulting film also has light barrier properties that protect food from photodegradation.

The optical properties of the gelatin/C-dots bio-nanocomposite films can also be observed with the fluorescence spectrum of the films (Figure 4b). The fluorescence spectrum of the gelatin/C-dots bio-nanocomposite film, excited at 400 nm, showed the emission intensity undergoing a redshift. Redshift occurred at 500 nm, 515 nm, and 517 nm as the amount of C-dots in the gelatin film increased. The redshift occurs probably because of the specific structure of nanoparticles, and the scattering phenomenon depends on the concentration of the nanoparticles⁸⁰. The structure and increase of the graphite carbon domain on the C-dots cause the redshift⁸¹. The redshift is also possible because of the irregularity of boundary polymer chains between nanoparticles and gelatin molecules. Thereby changing the environment of the tyrosine residue on the gelatin⁸².

4. CONCLUSIONS

In conclusion, this study successfully fabricated gelatin/C-dots bio-nanocomposite films with improved physicochemical, mechanical, thermal, and optical properties through the controlled incorporation of C-dots. The distinctive contribution of this work lies in the integrated evaluation of how interfacial interactions between gelatin and C-dots influence multiple functional attributes simultaneously, rather than enhancing a single property in isolation. The incorporation of C-dots resulted in a significant reduction in WVTR, increased density, and enhanced

mechanical performance without altering the fundamental chemical structure of the gelatin matrix, as confirmed by FTIR analysis and uniform nanoparticle dispersion observed in SEM images. These improvements provide practical evidence that the developed films possess sufficient barrier efficiency and mechanical integrity to support their application as active packaging materials during food storage and distribution. In addition, the improved thermal stability and fluorescence-related optical properties further extend the potential functionality of the films toward intelligent packaging applications. When compared with previously reported gelatin-based nanocomposite films, which predominantly emphasize individual enhancements, the gelatin/C-dots films developed in this study, particularly at 0.5% (w/w) C-dots, exhibit a more balanced combination of strength, flexibility, barrier performance, and multifunctionality at a relatively low nanofiller content. Overall, this study advances the understanding of structure–property–function relationships in gelatin-based bio-nanocomposite films with C-dots and supports their potential use in sustainable active and smart packaging systems.

ACKNOWLEDGMENTS

This study was funded by the LPDP RI (Rispro Invitasi LPDP RI) research project and the LPPM-HSC IPB Student Connectivity Program.

REFERENCES

- Nurilmala M, Darmawan N, Putri EAW, Jacob AM, Irawadi TT. Pangasius Fish Skin and Swim Bladder as Gelatin Sources for Hard Capsule Material. *Int J Biomater.* 2021;2021:1-6. doi:10.1155/2021/6658002
- Kandra R, Bajpai S. Synthesis, mechanical properties of fluorescent carbon dots loaded nanocomposites chitosan film for wound healing and drug delivery. *Arab J Chem.* 2020;13:4882-4894. doi:10.1016/j.arabjc.2019.12.010
- Abedinia A, Alimohammadi F, Teymori F, Razgardani N, Asl MRS, Ariffin F, Nafchi AM, Huda N, Roslan J. Characterization and cell viability of probiotic/prebiotics film based on duck feet gelatin: A novel poultry gelatin as a suitable matrix for probiotics. *Foods.* 2021;10(8):1-16. doi:10.3390/foods10081761
- Amjadi S, Emaminia S, Heyat Davudian S, Pourmohammad S, Hamishehkar H, Roufegarinejad L. Preparation and characterization of gelatin-based nanocomposite containing chitosan nanofiber and ZnO nanoparticles. *Carbohydr Polym.* 2019;216:376-384. doi:10.1016/j.carbpol.2019.03.062
- Kundu S, Das A, Basu A, Abdullah MF, Mukherjee A. Guar gum benzoate nanoparticle reinforced gelatin films for enhanced thermal insulation, mechanical and antimicrobial properties. *Carbohydr Polym.* 2017;170:89-98. doi:10.1016/j.carbpol.2017.04.056
- Nurilmala M, Suryamarevita H, Husein Hizbullah H, Jacob AM, Ochiai Y. Fish skin as a biomaterial for halal collagen and gelatin. *Saudi J Biol Sci.* 2021;(xxxx):1-11. doi:10.1016/j.sjbs.2021.09.056
- Shankar S, Teng X, Li G, Rhim JW. Preparation, characterization, and antimicrobial activity of gelatin/ZnO nanocomposite films. *Food Hydrocoll.* 2015;45:264-271. doi:10.1016/j.foodhyd.2014.12.001
- Hosseini SF, Rezaei M, Zandi M, Farahmandghavi F. Fabrication of bio-nanocomposite films based on fish gelatin reinforced with chitosan nanoparticles. *Food Hydrocoll.* 2015;44:172-182. doi:10.1016/j.foodhyd.2014.09.004
- Sarfraz J, Gulin-Sarfraz T, Nilsen-Nygaard J, Pettersen MK. Nanocomposites for food packaging applications: An overview. *Nanomaterials.* 2021;11(10):1-27. doi:10.3390/nano11010010
- Khusairy M, Rahman MR, Taib SNL, Khui PLN, Kakar A, Jayamani E. *Nano-Reinforcement in Sustainable Polymer Composites.* Woodhead Publishing; 2021. doi:10.1016/b978-0-12-820338-5.00010-2
- Roy S, Rhim JW. Gelatin-based film integrated with copper sulfide nanoparticles for active packaging applications. *Appl Sci.* 2021;11(14):1-12. doi:10.3390/app11146307
- Arfat YA, Ahmed J, Hiremath N, Auras R, Joseph A. Thermo-mechanical, rheological, structural and antimicrobial properties of bionanocomposite films based on fish skin gelatin and silver-copper nanoparticles. *Food Hydrocoll.* 2017;62:191-202. doi:10.1016/j.foodhyd.2016.08.009
- Wang H, Zhang M, Ma Y, Wang B, Huang H, Liu Y, Shao M, Kang Z, Huang H, Liu Y, Kang Z. Carbon Dots Derived from Citric Acid and Glutathione as a Highly Efficient Intracellular Reactive Oxygen Species Scavenger for Alleviating the Lipopolysaccharide-Induced Inflammation in Macrophages. *ACS Appl Mater Interfaces.* 2020;12(37):41088-41095. doi:10.1021/acsami.0c11735
- Zhou Y, Sharma SK, Peng Z, Leblanc RM. Polymers in carbon dots: A review. *Polymers (Basel).* 2017;9(2):67. doi:10.3390/polym9020067

15. Sreenath PR, Mandal S, Panigrahi H, Das P, Dinesh Kumar K. Carbon dots: Fluorescence active, covalently conjugated and strong reinforcing nanofiller for polymer latex. *Nano-Structures and Nano-Objects*. 2020;23:100477. doi:10.1016/j.nanoso.2020.100477
16. Dai Y, Wang J, Tao P, He R. Various hydrophilic carbon dots doped high temperature proton exchange composite membranes based on polyvinylpyrrolidone and polyethersulfone. *J Colloid Interface Sci*. 2019;553:503-511. doi:10.1016/j.jcis.2019.06.020
17. Yuan Z, Wu X, Jiang Y, Li Y, Huang J, Hao L, Zhang J, Wang J. Carbon dots-incorporated composite membrane towards enhanced organic solvent nanofiltration performance. *J Memb Sci*. 2018;549:1-11. doi:10.1016/j.memsci.2017.11.051
18. Dong Y, Wang R, Li H, Shao J, Chi Y, Lin X, Chen G. Polyamine-functionalized carbon quantum dots for chemical sensing. *Carbon N Y*. 2012;50(8):2810-2815. doi:10.1016/j.carbon.2012.02.046
19. Zhu S, Meng Q, Wang L, Zhang J, Song Y, Jin H, Zhang K, Sun H, Wang H, Yang B. Highly Photoluminescent Carbon Dots for Multicolor Patterning, Sensors, and Bioimaging. *Angew Chemie*. 2013;125(14):4045-4049. doi:10.1002/ange.201300519
20. Kasprzyk W, Świergosz T, Bednarz S, Walas K, Bashmakova N V., Bogdał D. Luminescence phenomena of carbon dots derived from citric acid and urea—a molecular insight. *Nanoscale*. 2018;10(29):13889-13894. doi:10.1039/c8nr03602k
21. Wang Y, Li Y, Xu Y. Synthesis of mechanical responsive carbon dots with fluorescence enhancement. *J Colloid Interface Sci*. 2020;560:85-90. doi:10.1016/j.jcis.2019.10.039
22. Long C, Jiang Z, Shangguan J, Qing T, Zhang P, Feng B. Applications of carbon dots in environmental pollution control: A review. *Chem Eng J*. 2021;406(2021):126848. doi:10.1016/j.cej.2020.126848
23. Wu B, Zhu G, Dufresne A, Lin N. Fluorescent Aerogels Based on Chemical Crosslinking between Nanocellulose and Carbon Dots for Optical Sensor. *ACS Appl Mater Interfaces*. 2019;11(17):16048-16058. doi:10.1021/acsami.9b02754
24. Syafei D, Sugiarti S, Darmawan N, Khotib M. Synthesis of TiO₂/carbon nanoparticle (C-dot) composites as active catalysts for photodegradation of persistent organic pollutant. *Indones J Chem*. 2017;17(1):37-42. doi:10.22146/ijc.23615
25. Anindita F, Darmawan N, Mas'Ud ZA. Fluorescence carbon dots from durian as an eco-friendly inhibitor for copper corrosion. *AIP Conf Proc*. 2018;(02008):1-7. doi:10.1063/1.5054412
26. Zhai X, Zou X, Shi J, Huang X, Sun Z, Li Z, Sun Y, Li Y, Wang X, Holmes M, Gong Y, Povey M, Xiao J. Amine-responsive bilayer films with improved illumination stability and electrochemical writing property for visual monitoring of meat spoilage. *Sensors Actuators, B Chem*. 2020;302(July 2019):127130. doi:10.1016/j.snb.2019.127130
27. Bhattacharyya SK, Dule M, Paul R, Dash J, Anas M, Mandal TK, Das P, Das NC, Banerjee S. Carbon Dot Cross-Linked Gelatin Nanocomposite Hydrogel for pH-Sensing and pH-Responsive Drug Delivery. *ACS Biomater Sci Eng*. 2020;6(10):5662-5674. doi:10.1021/acsbiomaterials.0c00982
28. Campalani C, Causin V, Selva M, Perosa A. Fish-Waste-Derived Gelatin and Carbon Dots for Biobased UV-Blocking Films. *ACS Appl Mater Interfaces*. 2022;14(30):35148-35156. doi:10.1021/acscami.2c11749
29. Sendão R, Yuso M del VM de, Algarra M, Esteves da Silva JCG, Pinto da Silva L. Comparative life cycle assessment of bottom-up synthesis routes for carbon dots derived from citric acid and urea. *J Clean Prod*. 2020;254:1-10. doi:10.1016/j.jclepro.2020.120080
30. Sugiarti S, Darmawan N. Synthesis of fluorescence carbon nanoparticles from ascorbic acid. *Indones J Chem*. 2015;15(2):141-145. doi:10.22146/ijc.21207
31. Geleta TT, Habtegebrel SA, Tolesa GN. Physical, mechanical, and optical properties of enset starch from bulla films influenced by different glycerol concentrations and temperatures. *J Food Process Preserv*. 2020;44(8):1-9. doi:10.1111/jfpp.14586
32. Pellá MCG, Silva OA, Pellá MG, Beneton AG, Caetano J, Simoes MR, Dragunski DC. Effect of gelatin and casein additions on starch edible biodegradable films for fruit surface coating. *Food Chem*. 2020;309:125764. doi:10.1016/j.foodchem.2019.125764
33. ISO 1183-1. *Plastics-Methods for Determining the Density of Non-Cellular Plastics*. ISO; 2019.
34. Akhavan-Kharazian N, Izadi-Vasafi H. Preparation and characterization of chitosan/gelatin/nanocrystalline cellulose/calcium peroxide films for potential wound dressing applications. *Int J Biol Macromol*. 2019;133:881-891. doi:10.1016/j.ijbiomac.2019.04.159

35. ASTM D882-12. *Standard Test Method for Tensile Properties of Thin Plastic Sheeting*. American Society for Testing and Materials; 2012.
36. Zhang X, Xu H, Li Y, Xu Y. Carbon-Dot-Based Thin Film with Responses toward Mechanical Stimulation and Acidic/Basic Vapors. *ACS Omega*. 2020;5(21):12144-12147. doi:10.1021/acsomega.0c00465
37. Yang Z, Chaieb S, Hemar Y. Gelatin-Based Nanocomposites: A Review. *Polym Rev*. 2021;61(4):765-813. doi:10.1080/15583724.2021.1897995
38. Procopio FR, Lourenço RV, Ana M, Bitante QB, Jose P, Ant M, Jachinto C. Sustainable Biopolymer Films from Amazonian Tambatinga Fish Waste : Gelatin Extraction and Performance for Food Packaging Applications. *foods*. 2025;14(3866):1-18.
39. Kavooosi G, Dadfar SMM, Dadfar SMA, Ahmadi F, Niakosari M. Investigation of gelatin/multi-walled carbon nanotube nanocomposite films as packaging materials. *Food Sci Nutr*. 2014;2(1):65-73. doi:10.1002/fsn3.81
40. Japanese Industrial Standard (JIS). *Japanese Industrial Standard*. 2 : 1707. Japanese Standards Association; 1975.
41. Shanmugam K, Doosthosseini H, Varanasi S, Garnier G, Batchelor W. Nanocellulose films as air and water vapour barriers: A recyclable and biodegradable alternative to polyolefin packaging. *Sustain Mater Technol*. 2019;22:e00115. doi:10.1016/j.susmat.2019.e00115
42. Khoirunnisa AR, Joni IM, Panatarani C, Rochima E, Praseptiangga D. UV-screening, transparency and water barrier properties of semi refined iota carrageenan packaging film incorporated with ZnO nanoparticles. *AIP Conf Proc*. 2018;1927(030041):1-7. doi:10.1063/1.5021234
43. Atarés L, Chiralt A. Essential oils as additives in biodegradable films and coatings for active food packaging. *Trends Food Sci Technol*. 2016;48:51-62. doi:10.1016/j.tifs.2015.12.001
44. Andrade MA, Barbosa CH, Ribeiro-santos R, Tome S, Fernando AL, Silva AS, Vilarinho F. Emerging Trends in Active Packaging for Food: A Six-Year Review. *Foods*. 2025;14(2713):1-43.
45. Liu J, Li R, Yang B. Carbon Dots: A New Type of Carbon-Based Nanomaterial with Wide Applications. *ACS Cent Sci*. 2020;6(12):2179-2195. doi:10.1021/acscentsci.0c01306
46. Kan J, Li M, Liu M, Jiang N, Yue Z, Yu H, Sun R. Interfacial Engineering of High-Performance Pickering Emulsion – Gelatin Composite Films for Active Packaging. *Foods*. 2025;14(3978):1-26.
47. Nuvoli L, Conte P, Fadda C, Ruiz R, Garcia M, Baldino S, Mannu A. Structural , thermal , and mechanical properties of gelatin-based films integrated with tara gum. *Polymer (Guildf)*. Published online 2020:1-9. doi:10.1016/j.polymer.2020.123244
48. Zhou E, Xi J, Guo Y, Liu Y, Xu Z, Peng L, Gao W, Ying J, Chen Z, Gao C. Synergistic effect of graphene and carbon nanotube for high-performance electromagnetic interference shielding films. *Carbon N Y*. 2018;133:316-322. doi:10.1016/j.carbon.2018.03.023
49. Ilyas RA, Sapuan SM, Ibrahim R, Abrar H, Ishak MR, Zainudin ES, Atikah MSN, Mohd Nurazzi N, Atiqah A, Ansari MSN, Syafri E, Asrofi M, Sari NH, Jumaidin R. Effect of sugar palm nanofibrillated cellulose concentrations on morphological, mechanical and physical properties of biodegradable films based on agro-waste sugar palm (*Arenga pinnata* (Wurmb.) Merr) starch. *J Mater Res Technol*. 2019;8(5):4819-4830. doi:10.1016/j.jmrt.2019.08.028
50. Boateng J, Khan S. Composite HPMC-Gelatin Films Loaded with Cameroonian and Manuka Honeys Show Antibacterial and Functional Wound Dressing Properties. *gels*. 2025;11(557):1-23.
51. Shrungi M, Goswami A, Bajpai J, Bajpai AK. Designing kaolin-reinforced bionanocomposites of poly(vinyl alcohol)/gelatin and study of their mechanical and water vapor transmission behavior. *Polym Bull*. 2019;76(11):5791-5811. doi:10.1007/s00289-019-02684-4
52. Haghghi H, De Leo R, Bedin E, Pfeifer F, Siesler HW, Pulvirenti A. Comparative analysis of blend and bilayer films based on chitosan and gelatin enriched with LAE (lauroyl arginate ethyl) with antimicrobial activity for food packaging applications. *Food Packag Shelf Life*. 2019;19(November 2018):31-39. doi:10.1016/j.fpsl.2018.11.015
53. Meindrawan B, Suyatma NE, Wardana AA, Pamela VY. Nanocomposite coating based on carrageenan and ZnO nanoparticles to maintain the storage quality of mango. *Food Packag Shelf Life*. 2018;18(November 2017):140-146. doi:10.1016/j.fpsl.2018.10.006
54. Binaymotlagh R, Chronopoulou L, Palocci C. An Overview of Biopolymer-Based Graphene Nanocomposites for Biotechnological Applications. *Materials (Basel)*. 2025;18(2978):1-35.

55. Shankar S, Wang LF, Rhim JW. Effect of melanin nanoparticles on the mechanical, water vapor barrier, and antioxidant properties of gelatin-based films for food packaging application. *Food Packag Shelf Life*. 2019;21(January):100363. doi:10.1016/j.fpsl.2019.100363
56. Ahammed S, Liu F, Khin MN, Yokoyama WH, Zhong F. Improvement of the water resistance and ductility of gelatin film by zein. *Food Hydrocoll*. 2020;105:105804. doi:10.1016/j.foodhyd.2020.105804
57. Nilsuwan K, Benjakul S, Prodpran T. Properties and antioxidative activity of fish gelatin-based film incorporated with epigallocatechin gallate. *Food Hydrocoll*. 2018;80:212-221. doi:10.1016/j.foodhyd.2018.01.033
58. Wu X, Tong Z, Liu Y, Yang Y, Li Y, Cheng Y, Yu J, Liu N. Cationic carbon dots: A novel class of mimetic enzymes. *Nano Res*. 2025;18(94907333):1-23.
59. Cazón P, Velazquez G, Ramírez JA, Vázquez M. Polysaccharide-based films and coatings for food packaging: A review. *Food Hydrocoll*. 2017;68:136-148. doi:10.1016/j.foodhyd.2016.09.009
60. Sentanin L, Gonçalves J, Filho DO, Egea MB, Henrique L, Mattoso C. Smart and Mechanically Enhanced Zein – Gelatin Films Incorporating Cellulose Nanocrystals and Alizarin for Fish Spoilage Monitoring. *Foods*. 2025;14(3015):1-18.
61. American Society for Testing and Materials. ASTM. Standard test methods for tensile properties of thin plastic sheeting, method D882-10. *Annu B ASTM Stand*. 2010;87(Reapproved):3-5. doi:10.1520/D0882-10.2
62. Loo CPY, Sarbon NM. Chicken skin gelatin films with tapioca starch. *Food Biosci*. 2020;35(100589):1-8. doi:10.1016/j.fbio.2020.100589
63. Bang Y, Shankar S, Rhim J. In situ synthesis of multi-functional gelatin / resorcinol / silver nanoparticles composite films. *Food Packag Shelf Life*. 2019;22(July):100399. doi:10.1016/j.fpsl.2019.100399
64. Nagarajan M, Benjakul S, Prodpran T, Songtipya P. Characteristics of bio-nanocomposite films from tilapia skin gelatin incorporated with hydrophilic and hydrophobic nanoclays. *J Food Eng*. 2014;143:195-204. doi:10.1016/j.jfoodeng.2014.06.038
65. Sahraee S, Ghanbarzadeh B, Milani JM, Hamishehkar H. Development of Gelatin Bionanocomposite Films Containing Chitin and ZnO Nanoparticles. *Food Bioprocess Technol*. 2017;10(8):1441-1453. doi:10.1007/s11947-017-1907-2
66. Leta TB, Adeyemi JO, Fawole OA. Carbon Dot Nanoparticles Synthesized from Horticultural Extracts for Postharvest Shelf-Life Extension of Fruits and Vegetables. *Plants*. 2025;14(2523):1-51.
67. León-lópez A, Flores-gutiérrez EV, Cenobio-galindo ADJ, Islas-moreno A. Gelatin-Based Films Containing Extracts of Prickly Pear (*Opuntia guerrana*): Characterization and Evaluation of Bioactive Properties. *Foods*. 2025;14(3911):1-16.
68. Augusto V, Rodrigues GDM, Monteiro VM, Carvalho RAD, Silva C, Maria C, Yoshida P, Martelli SM, Velasco JI, Fakhouri FM. A Gelatin-Based Film with Acerola Pulp: Production, Characterization, and Application in the Stability of Meat Products. *Polymers (Basel)*. 2025;17(1882):1-15.
69. Sultan M, Ibrahim H, Mohammed H, Masry E, Hassan YR. Antimicrobial gelatin - based films with cinnamaldehyde and ZnO nanoparticles for sustainable food packaging. *Sci Rep*. 2024;24(24499):1-21. doi:10.1038/s41598-024-72009-7
70. Fonseca J de M, Valencia GA, Soares LS, Dotto MER, Campos CEM, Moreira RDFPM, Fritz ARM. Hydroxypropyl methylcellulose-TiO₂ and gelatin-TiO₂ nanocomposite films: Physicochemical and structural properties. *Int J Biol Macromol*. 2020;151:944-956. doi:10.1016/j.ijbiomac.2019.11.082
71. Azizi-Lalabadi M, Alizadeh-Sani M, Divband B, Ehsani A, McClements DJ. Nanocomposite films consisting of functional nanoparticles (TiO₂ and ZnO) embedded in 4A-Zeolite and mixed polymer matrices (gelatin and polyvinyl alcohol). *Food Res Int*. 2020;137:109716. doi:10.1016/j.foodres.2020.109716
72. Castro MCR, André MP, Pereira P, Cruz V, Machado AV, Rodrigues PV. Tailoring PLA / Gelatin Film Properties for Food Packaging Using Deep Eutectic Solvents. *Molecules*. 2026;31(39):1-17.
73. Rubini K, Menichetti A, Cassani MC, Montalti M, Bigi A, Boanini E. The Role of WO₃ Nanoparticles on the Properties of Gelatin Films. *gels*. 2024;10(354):1-15.
74. Shankar S, Teng X, Rhim J. Effects of concentration of ZnO nanoparticles on mechanical, optical, thermal, and antimicrobial properties of gelatin/ZnO nanocomposite Films. *Korean J Packag Sci Technol*. 2014;20(2):41-49.
75. Riahi Z, Priyadarshi R, Rhim J, Bagheri R. Food Hydrocolloids Gelatin-based functional films

- integrated with grapefruit seed extract and TiO₂ for active food packaging applications. *Food Hydrocoll.* 2021;112(September 2020):106314. doi:10.1016/j.foodhyd.2020.106314
76. Bai R, Zhang X, Yong H, Wang X, Liu Y, Liu J. Development and characterization of antioxidant active packaging and intelligent Al³⁺-sensing films based on carboxymethyl chitosan and quercetin. *Int J Biol Macromol.* 2019;126(2019):1074-1084. doi:10.1016/j.ijbiomac.2018.12.264
77. Tavassoli M, Alizadeh M, Khezerlou A, Ehsani A, Julian D. Food Hydrocolloids Multifunctional nanocomposite active packaging materials: Immobilization of quercetin, lactoferrin, and chitosan nanofiber particles in gelatin films. *Food Hydrocoll.* 2021;118(March):106747. doi:10.1016/j.foodhyd.2021.106747
78. Kavooosi G, Rahmatollahi A, Mohammad Mahdi Dadfar S, Mohammadi Purfard A. Effects of essential oil on the water binding capacity, physico-mechanical properties, antioxidant and antibacterial activity of gelatin films. *LWT - Food Sci Technol.* 2014;57(2):556-561. doi:10.1016/j.lwt.2014.02.008
79. Kanmani P, Rhim JW. Properties and characterization of bionanocomposite films prepared with various biopolymers and ZnO nanoparticles. *Carbohydr Polym.* 2014;106(1):190-199. doi:10.1016/j.carbpol.2014.02.007
80. Li X, Wang W, Li Q, Lin H, Xu Y, Zhuang L. Design of Fe₃O₄@SiO₂@mSiO₂-organosilane carbon dots nanoparticles: Synthesis and fluorescence red-shift properties with concentration dependence. *Mater Des.* 2018;151(2017):89-101. doi:10.1016/j.matdes.2018.04.051
81. Ren J, Malfatti L, Innocenzi P. Citric Acid Derived Carbon Dots, the Challenge of Understanding the Synthesis-Structure Relationship. *J Carbon Res.* 2020;7(1):2. doi:10.3390/c7010002
82. He Q, Zhang Y, Cai X, Wang S. Fabrication of gelatin-TiO₂ nanocomposite film and its structural, antibacterial and physical properties. *Int J Biol Macromol.* 2016;84:153-160. doi:10.1016/j.ijbiomac.2015.12.012